New measuring method of fiber alignment in precision torsion pendulum experiments*

Bing-Jie Wang(王冰洁), Li Xu(徐利), Wei-You Zeng(曾维友), and Qing-Lan Wang(王晴岚)†

College of Science, Hubei University of Automotive and Technology, Shiyan 442002, *China*

(Received 20 March 2020; revised manuscript received 27 April 2020; accepted manuscript online 27 May 2020)

Testing the extreme weak gravitational forces between torsion pendulum and surrounding objects will indicate new physics which attracts many interests. In these measurements, the fiber alignment plays a crucial role in fulfilling high precision placement measurement, especially in measuring the deviation between the fiber and source mass or other objects. The traditional way of the fiber alignment requires to measure the component of the pendulum body and then transfer to the torsion fiber by some complicated calculations. A new method is reported here by using a CCD camera to get the projection image of the torsion fiber, which is a direct and no-contact measurement. Furthermore, the relative position change of the torsion fiber can also be monitored during the experiment. In our experiment, the alignment between the fiber and the center of the turntable has been operated as an example. Our result reaches the accuracy of several micrometers which is higher than the previous method.

Keywords: torsion pendulum, alignment, CCD camera

PACS: 04.80.Cc **DOI:** 10.1088/1674-1056/ab969d

1. Introduction

Torsion pendulum is adopted in most of gravitational force detections,[1] such as Newtonian Inverse Square Law violation test,[2,3] equivalence principle test,[4–6] Newtonian constant G measurement,[7–9] and gravitational reference sensor testing bed for the gravitational wave detect missions.[10,11] Especially in the Newtonian constant G measurement experiment, a pendulum suspended by a very thin fiber is to measure the gravitational torque caused by the source masses around. The time-of-swing method and angular-acceleration-feedback method are adopted in G measurement mostly. The source masses are put on a turntable which rotates with the torsion pendulum coaxially to produce or reduce the tiny change of the gravitational torque. Since G is an absolute measurement value, the calculation of the gravitational torque change driven by the turntable must be taken very carefully. The alignment between the torsion fiber and turntable becomes a very important issue.

The previous way of torsion fiber alignment in Ref. [12] mentioned that an infrared detector was adopted to fixed on the turntable at first. Since the fiber is too thin to be measured by the infrared detector, the detector is used to measure the position of the clamp which is attached firmly on top of the pendulum instead. After recording the output of the infrared detector at four edges, the deviation between the turntable rotating axis and the torsion fiber can be inferred through some complicated calculation. This kind of measurement is indirect and all the operations are executed in air. The position of the torsion fiber might shift a little bit when in the vacuum condition which is caused by the deformation of the vacuum chamber and it is hard to be detected again. Therefore, measuring, aligning, and monitoring of the torsion fiber become an important step to guarantee the correctness and reliableness of the experiment.

In this paper, a novel optical measurement method is introduced to detect the relative position between the torsion fiber and the center of the turntable directly. Furthermore, all the implementations are operated non-contact. The position change of the torsion fiber is seized by a CCD camera and analyzed by image processing to achieve the precise position. The deviation between the fiber and the turntable is measured directly without transferring. The uncertainty of this method reaches an accuracy of several micrometers which is dependent on the pixel size of the CCD camera and the stableness of the environment. One can use this system to monitor the position change of the fiber during the experiment procedure. It is also suitable for the rotation-like experiment[13,14] or where the center of a turntable needs to be determined.[15,16]

2. Experimental setup

Alignment with the torsion fiber and the turntable in Newtonian constant G measurement[12] is set as an example here to describe the new method in detail, as shown schematically in Fig. 1. A collimated laser beam and a CCD camera are mounted on the turntable, standing on the opposite sides to get the projection image of the torsion fiber. The top end of

*Project supported by the National Natural Science Foundation of China (Grant No. 11305057).

†Corresponding author. E-mail: qinglanwang@126.com

the fiber is glued to a two-axis stage which is fixed to a stable optical table shelf. The bottom of the fiber is connected with a simple pendulum which is suspended near the center of the turntable, initially.

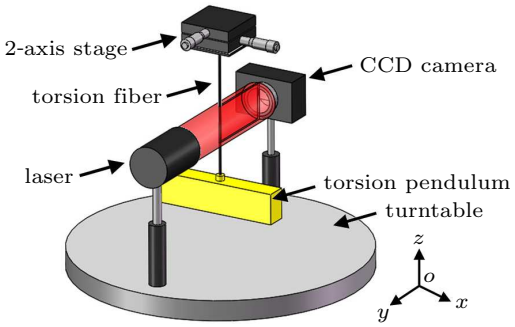

Fig. 1. A schematic drawing of the setup. The laser with large beam incidents into the CCD camera. Both of them are fixed on the turntable and rotated with it. The top of the fiber is fixed to a two-axis stage which is used to adjust the position of the fiber.

When the turntable rotates, the CCD camera will get a serial of photos to show the projection of the fiber. Figure 2 shows the images in each 10° while the stage rotates for 360°. If the fiber is exactly at the center of the turntable, the position of the project image will not change. Otherwise, it will change regularly. By analyzing the images to get the relative position between the fiber and the center of the turntable, then use the two-axis stage to move the fiber close to the center of the turntable step by step.

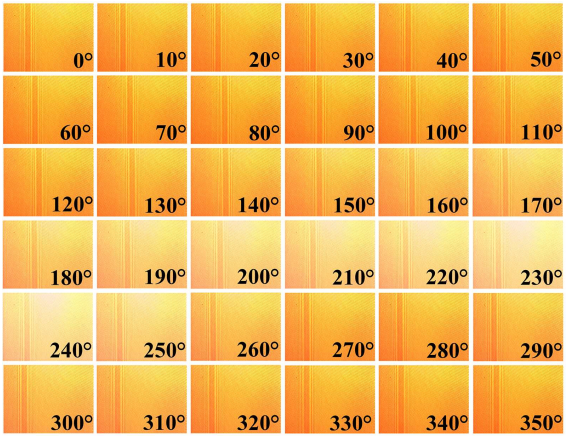

Fig. 2. A serial projection images of the fiber are shown when the turntable rotates in 360°. The regularly changed position means that there exists a deviation between the fiber and the center of the turntable.

3. Data analysis

3.1. Image processing

The diameter of the torsion fiber is about several decades or hundreds micrometers, which leads to the straight edge diffraction effect in this experiment.[17] Figure 3(a) shows the original image of the fiber which is adopted in our experiment, the diameter of the fiber is 25 μm. The edge of the shadow is not at the edge of the fiber, but some distance away from it. The intensity of the diffraction pattern is situated at a distance from the edge of the fiber.

The original image is converted to a grayscale intensity image, then adjusted to enhance the contrast of the image as shown in Fig. 3(b). The bright pixel is set as 0, while the dark one as 1.[18] When the values of grayscale summarized by column, the position and diffraction pattern of the fiber are shown in Fig. 4(a). The center of the fiber is near No. 900 pixel, the patterns besides the fiber are caused by the straight edge diffraction which fulfills the equation as follows:[19]

$$I_{\mathrm{r}} = \frac{1}{2}\left\{\left[\frac{1}{2}+\int_0^{\omega}\cos\left(\frac{\pi}{2}\tau^2\right)\mathrm{d}\tau\right]^2 + \left[\frac{1}{2}+\int_0^{\omega}\sin\left(\frac{\pi}{2}\tau^2\right)\mathrm{d}\tau\right]^2\right\}, \tag{1}$$

where I_{r} represents the relative diffraction intensity, and $\omega = \sqrt{(2/\lambda s')}u$ in which s' is the distance between the fiber and the CCD sensor while u is the coordinate of the intensity distribution on the receiving screen.

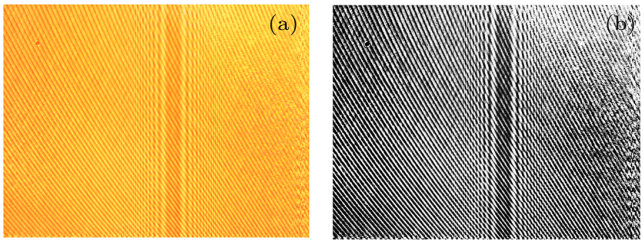

Fig. 3. Projection image of the fiber. The intensity distribution can be explained by Fresnel diffraction pattern of a straight edge: (a) original image and (b) enhanced grayscale intensity image.

The position information of the center of the fiber depends on the edge detection. Fitting the curve by using the function with Eq. (1) will get the information of the shape and position of the fiber. Many parameters in the function need to be fitting correctly which will lead to tough and complicated numerical calculations. Fortunately, the true edge of the fiber is not a critical factor in this experiment. It is not necessary to point out the geometrical shape of the fiber, but the change of the fiber center. A more simple way is introduced here to get the position of the center of the fiber while ignores the true edge detection.

In the image processing domain, a variety of ways to detect objective's edge have been discussed a lot in Refs. [20,21]. The Canny algorithm framework is chosen because it has the advantages of no sensitivity to the noise, high resolution, and depressing the false edge detection.[22] It will find the edge by searching for local maximum of the change of the specified range $f[x_{mi}, R_{mi}]$ in Fig. 4(b), where R_{mi} is the magnitude of the summarized grayscale, $x_{mi} = x_{m(-n)}, x_{m(-n+1)}, \ldots, x_{m(n-1)}, x_{m(n)}$ is the highlight range

which is chosen manually, m is the sequence number of the image in different angles and i is the number of the pixel in each image.[23] We focus on the nearest range besides the central part as shown in Fig. 4(b). The change between two contiguous points is calculated as follows:

$$\begin{aligned} \Delta_{mi(\text{left})} &= R_{m(i-1)} - R_{mi}, \\ \Delta_{mi(\text{right})} &= R_{m(i+1)} - R_{mi}. \end{aligned} \tag{2}$$

Once the maximum change points have been determined as $x_{m\text{left}}$ and $x_{m\text{right}}$ in the left range and right range, the center of the torsion fiber in the m-th image is $x_m = (x_{m\text{left}} + x_{m\text{right}})/2$.

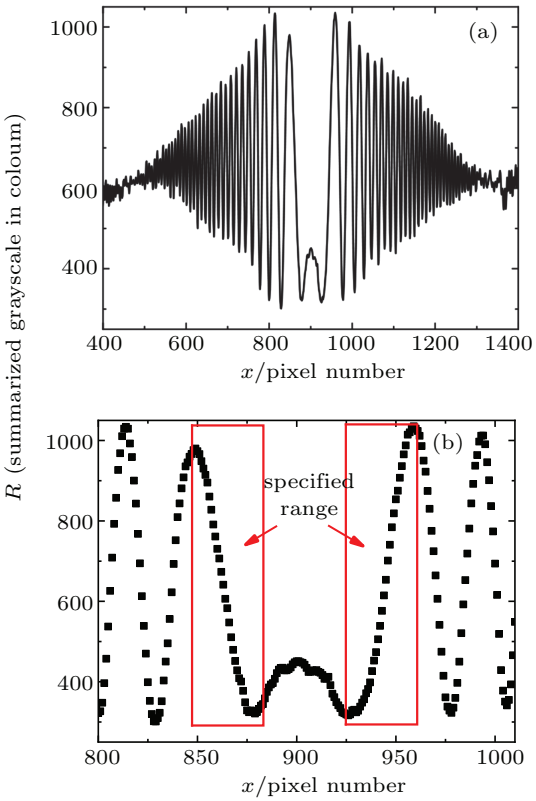

Fig. 4. (a) Summarizing the grayscale by column to get the distribution in the horizonal direction. The diffraction pattern shows symmetrically besides the two edges. (b) Searching the local maximum change in the manual chosen range to determine the center of the torsion fiber.

3.2. Data processing

A Cartesian coordinate system o–xyz is associated with the center of the turntable, z axis is along the rotating axis of the turntable, x axis is parallel to the screen of the CCD camera, and y axis is defined by the right-handed coordinate system shown in Fig. 5(a). The deviation and orientation between the fiber and the center of the turntable could be described by the function $x_m = D + r\cos(\beta + \theta_m)$, where D represents the pixel number of the center of the turntable shown in the image, r is the distance from the center of the turntable to the torsion fiber, β is the orientation angle, and $\theta_m = 10°, 20°, \ldots$ $(m = 1, 2, \ldots)$. The fitting result by means of 36 images from the CCD camera rotates for a circle is shown in Fig. 5(b). The deviation could be written as $\Delta x = r\cos\beta$ and $\Delta y = r\sin\beta$ in x and y directions, respectively.

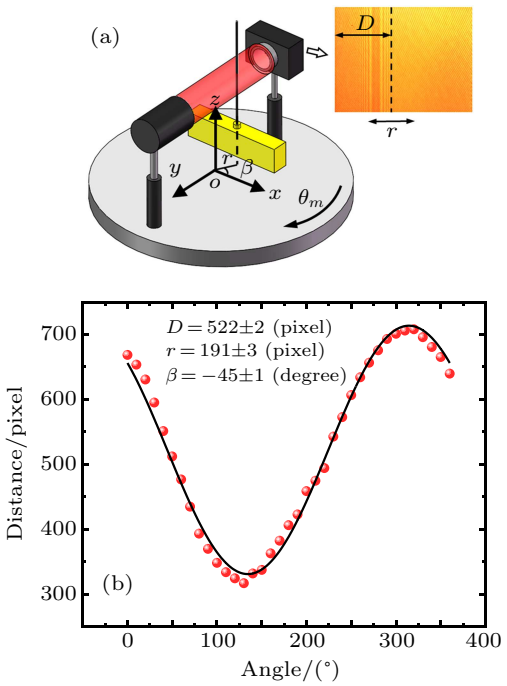

Fig. 5. (a) Schematic diagram of the system. By means of 36 images, the deviation result can be calculated. (b) The circle dots represent the deviation in each image obtained by the CCD camera in different angle locations. A sinusoidal curve function is used to fitting the data well. One can get more images in each angle to make the fitting result more precisely, but it is not improved significantly.

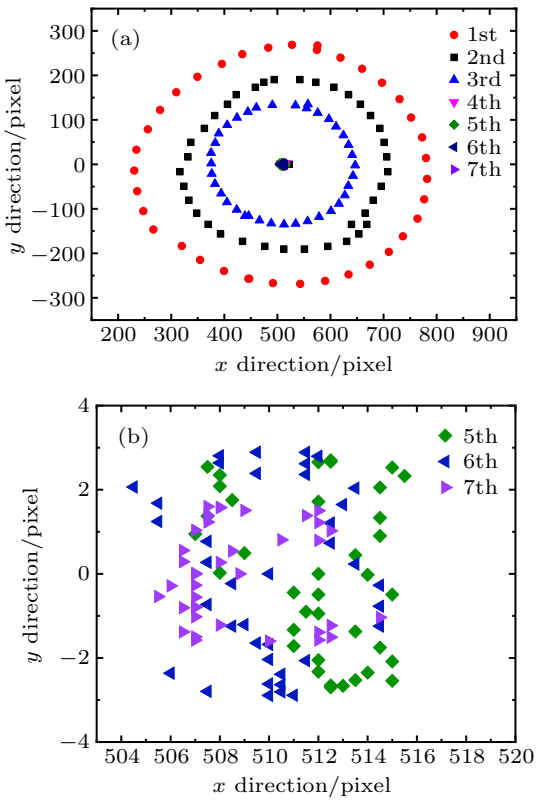

Fig. 6. (a) A serial results have been presented. The circles are getting smaller and smaller after several operations. (b) The last three operations seem to reach the same level.

According to the fitting result above, it is easy to recover the data to present the variation of the serial images. The torsion fiber (or the turntable) can be adjusted by the two-axis stage. After repeating the measurement several times, the deviation becomes smaller and smaller as shown in Fig. 6(a). In Fig. 6(b), the results from the last three measurements show that the distribution becomes randomly more than a circle. It seems the system is in the best situation we can achieve right now. One reason is that all the implements are installed on an optical table in the air which yields that the influence caused by the air flow and vibration can not be isolated well enough. The second reason is that the two-axis stage used for adjusting the position of the fiber is manual-operated which is difficult to reach a high precise level. The third one is the resolution of the CCD camera limits the uncertainties. The coefficients in the fitting function are shown in Table 1. It should be noted that the number of the pixel is used here in unit to describe the deviation result.

Table 1. Coefficients of the fitting function in deviation measurement.

	r/pixel	β/(°)	Δx/pixel	Δy/pixel	D/pixel
1st	269 ± 5	-107 ± 1	-79 ± 5	-257 ± 5	518 ± 3
2nd	191 ± 3	-45 ± 1	135 ± 3	-135 ± 3	522 ± 2
3rd	135 ± 2	239 ± 1	-70 ± 2	-116 ± 2	511 ± 1
4th	3 ± 1	-11 ± 8	3 ± 1	-1 ± 1	512 ± 3
5th	2 ± 1	-210 ± 18	-2 ± 1	-1 ± 1	509 ± 1
6th	3 ± 1	-25 ± 8	3 ± 1	-1 ± 1	510 ± 1

4. Results and discussion

The turntable used in the experiment is Daheng Optics GCD 011130M. The distance between the laser and fiber is about 30 mm, and the distance between the CCD camera and fiber is almost the same. The sensor of the camera (DAHENG IMAGING DH-SV2001FC) is 1628 pixels by 1236 pixels. The size of the pixel is 4.4 μm×4.4 μm given by the data sheet which should be calibrated carefully. A Piezo stage KPZ05/NFL5DP20 from Thorlab is adopted to calibrate the size of the pixel. The moving range of the Piezo stage is 20 μm and the resolution is 0.6 nm. In the calibration step, the CCD camera is fixed on the Piezo stage, the direction of the movement is perpendicular to the laser beam. Since the distance from the fiber to the camera is about 30 mm which is much lager compared with the moving range of the Piezo stage. A little bit offset in perpendicular direction can be ignored. The camera takes a photo in every 2.67 μm to record the projection of the torsion fiber. These images are analyzed in the same way as mentioned in Section 3. The calibration result is shown in Fig. 7, and the inherent effect of the hysteresis is included. The coefficient in terms of the calibration is (4.0 ± 0.3) μm/pixel. The final result of the deviation between the center of the torsion fiber and turntable is $\Delta x=(12.0\pm2.2)$ μm and $\Delta y=(-4.0\pm2.0)$ μm. Comparing with the result mentioned in Ref. [12], the uncertainties of the alignment fiber are 19 μm and 22 μm in the x and y directions, respectively. Our new method is better.

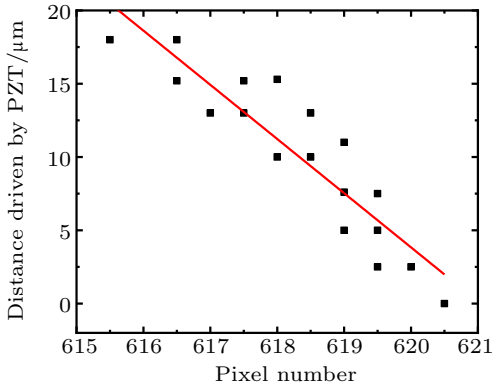

Fig. 7. The distance driven by the Piezo stage *versus* the information got from the image processing. The points in this figure are analyzed in the same way of image processing mentioned in Section 3.

There are some effects should be discussed here, such as the tilt and wobble of the turntable. Tilt means the rotating axis of the turntable is not in the vertical direction as the torsion fiber, while wobble is the wagging of the rotating axis during the turntable rotating as shown in Fig. 8(a). In order to figure out the extent of these effects, a transfer matrix is introduced here to describe the relationship between the turntable and torsion fiber (torsion pendulum) coordinates.

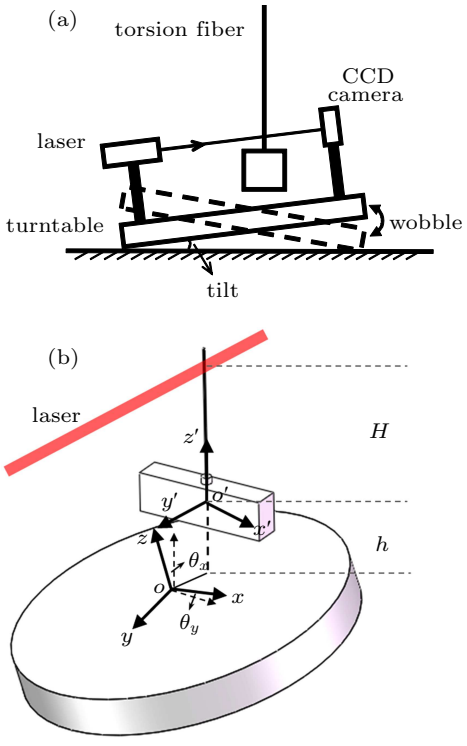

Fig. 8. (a) Scheme of the tilt and wobble motion during the experiment. (b) Two separated coordinates are used to describe the effects by the tilt and wobble. The height from the laser to the plane of the turntable is $h+H$.

A new coordinate system o'–$x'y'z$ is defined for the torsion pendulum. In this system, o' is the mass center of the pendulum as one usually does, x' is almost parallel to the x at the beginning, z' axis points along the torsional fiber and y' is given by the right-hand rule. The coordinate vectors are defined as $(\widehat{ex},\widehat{ey},\widehat{ez})$ and $(\widehat{ex'},\widehat{ey'},\widehat{ez'})$ for the turntable and the torsion pendulum system, respectively. The distance r from the center of the turntable o to the fiber is shown in Fig. 8(b), h represents the height from o' to the plane of turntable and H is the height of incident beam in o'–$x'y'z$ coordinate system. Considering the tilt and wobble effect, there are two angles shifts marked as θ_x between x and x', θ_y between y and y' which are very small. Tilt can be described as stable values of θ_x and θ_y, while variable values of θ_x and θ_y mean wobble. The transfer matrix between the two coordinates is written as follows:

$$\begin{pmatrix}\widehat{ex}\\ \widehat{ey}\\ \widehat{ez}\end{pmatrix} = \begin{pmatrix}\cos\theta_y & 0 & -\sin\theta_y\\ \sin\theta_x\sin\theta_y & \cos\theta_x & \cos\theta_y\sin\theta_x\\ \cos\theta_x\sin\theta_y & \sin\theta_x & \cos\theta_y\cos\theta_x\end{pmatrix} \times \begin{pmatrix}\cos\theta_m & -\sin\theta_m & 0\\ \sin\theta_m & \cos\theta_m & 0\\ 0 & 0 & 1\end{pmatrix}\begin{pmatrix}\widehat{ex'}\\ \widehat{ey'}\\ \widehat{ez'}\end{pmatrix}. \quad (3)$$

The details of the calculation can be found in Ref. [24]. Since we focus on the image which is parallel to the oxz plane, the coupled terms in x axis are analyzed here. Based on Eq. (3), θ_y is a small angle, the position of the torsion fiber is written as

$$\begin{aligned} x &= r\cos\theta_y\cos(\beta+\theta_m)-(h+H)\sin\theta_y \\ &\simeq r\left(1-\frac{\theta_y^2}{2}\right)\cos(\beta+\theta_m)-(h+H)\theta_y. \end{aligned} \quad (4)$$

In most of the torsion pendulum experiments, the existences of θ_x and θ_y will introduce many other serious side effects. These two angles should be measured, minimized, and controlled by some high precision instruments as low as 20 μrad in Ref. [8] and 3 nrad in Ref. [9]. An approximately estimation of the error is $\delta x = 2$ μm when the height from the incident laser to the turntable $h+H$ is 100 mm and the angle θ_y is 20 μrad in our experiment. It is noticed that the higher the incident laser beam, the larger the error will be coupled by the tilt and wobble effects.

Another phenomenon should be pointed out is that the torsion fiber is not straight enough as shown in Fig. 2. First, the pendulum used here is a 4.5-g block made with PLA material. However, for a 25-μm tungsten fiber, the suitable load should be about 80 g. Limited by our experimental conditions, a light pendulum made by 3D printer for convenience is used, which makes the torsion fiber not straight. Second, this phenomenon can also arise from the tilt and wobble which is discussed above. The third factor is the air flow makes the torsion fiber swing which is hard to be decreased.

Nevertheless, the diffraction information in each image is concentrated into one spot, and then it is fitted into a sinusoidal function by 36 spots from a serial images. The errors can be enlarged as $\Delta x = 0 \pm \sqrt{12.0^2+2.2^2}$ μm and $\Delta y = 0 \pm \sqrt{4.0^2+2.0^2}$ μm for insurance.

For the future improvements, all the system can be manipulated in an inclosed space, such as in the vacuum chamber to decrease the vibration and the air flow. A higher resolution camera with smaller pixel in size will improve the accuracy significantly. Motorized stage is also helpful for adjusting the fiber much more precisely to the specified position. In the image processing, a more convenient program with automatic range searching and analyzing will speed up the procedure. In addition, a lot of details should be investigated in the image processing. For example, the radius change of the fiber could be extracted from the diffraction pattern.

In conclusion, a novel scheme is introduced in our paper to monitor the torsion fiber by a CCD camera. The projection image of the fiber obtained by the camera is analyzed by image processing and the relative position variation of the fiber could be detected easily with high accuracy. It is convenient to use the new method to fulfill the alignment requirement. The accuracy in our experiment reported here increases significantly, and it may be improved in the future.

Acknowledgment

We are grateful to Gerhard Heinzel and Guy Apelbaum of Albert Einstein Institute for their valuable discussions and suggestions.

References

[1] Adelberger E G, Gundlach J H, Heckel B R, Hoedl S and Schlamminger S 2009 *Prog. Particle Nucl. Phys.* **62** 102
[2] Lee J G, Adelberger E G, Cook T S, Fleischer S M and Heckel B R 2020 *Phys. Rev. Lett.* **124** 101101
[3] Tan W H, Du A B, Dong W C, Yang S Q, Shao C G, Guan S G, Wang Q L, Zhan B F, Luo P S, Tu L C and Luo J 2020 *Phys. Rev. Lett.* **124** 051301
[4] Schlamminger S, Choi K Y, Wagner T A, Gundlach J H and Adelberger E G 2008 *Phys. Rev. Lett.* **100** 041101
[5] Xu J H, Shao C G, Luo J, Liu Q, Zhu L and Zhao H H 2017 *Chin. Phys. B* **26** 080401
[6] Zhu L, Liu Q, Zhao H H, Gong Q L, Yang S Q, Luo P S, Shao C G, Wang Q L, Tu L C and Luo J 2018 *Phys. Rev. Lett.* **121** 261101
[7] Quinn T 2000 *Nature* **408** 919
[8] Rothleitner C and Schlamminger S 2017 *Rev. Sci. Instrum.* **88** 111101
[9] Li Q, Xue C, Liu J P, Wu J F, Yang S Q, Shao C G, Quan L D, Tan W H, Tu L C, Liu Q, Xu H, Liu L X, Wang Q L, Hu Z K, Zhou Z B, Luo P S, Wu S C, Milyukov V and Luo J 2018 *Nature* **560** 582

[10] Bassan M, Cavalleri A, Laurentis M, Marchi F D, Rosa R D, Fiore L D, Dolesi R, Finetti N, Garufi, Grado A, Hueller M, Marconi L, Milano L, Pucacco G, Stanga R, Visco M, Vitale S and Weber W J 2016 *Phys. Rev. Lett.* **116** 051104

[11] Ciani G, Chilton A, Apple S, Olatunde T, Aitken M, Mueller G and Conklin J W 2017 *Rev. Sci. Instrum.* **88** 064502

[12] Tu L C, Li Q, Wang Q L, Shao C G, Yang S Q, Liu L X, Liu Q and Luo J 2010 *Phys. Rev. D* **82** 022001

[13] Ciani G 2008 *Free-fall of LISA Test Masses: a new torsion pendulum to test translational acceleration*, Ph.D. Dissertation (Trento: University of Trento)

[14] Huarcaya V, Apelbaum G, Haendchen V, Wang Q, Heinzel G and Mehment M 2020 *Class. Quantum Grav.* **37** 025004

[15] Kapner D J 2005 *A Short-Range of Newton's Gravitational Invers-Square Law*, Ph.D. Dissertation (Seattle: University of Washington)

[16] Wagner T A 2013 *Rotating Torsion Balance Tests of the Weak Equivalence Principle*, Ph.D. Dissertation (Seattle: University of Washington)

[17] Nityananda R 2015 *Resonance* **20** 389

[18] Blackledge J M 2005 *Digital Image Processing* (Chichester: West Sussex)

[19] Born M and Wolf E 1999 *Principles of Optics*, 7th edn. (Cambridge: Cambridge University Press)

[20] Biswas R and Sil J 2012 *Procedia Technology* **4** 820

[21] Gu J, Pan Y and Wang H 2015 *Optik* **126** 2974

[22] Canny J 1986 *IEEE Trans. Pattern Anal. Machine Intell.* **6** 679

[23] Ruslau M F V, Pratama R A, Nurhayati and Asmal S 2019 *Earth and Environmental Science* **343** 012198

[24] Liu Q 2009 *The precision measurement of Newtonian gravitational constant G by using double spherical source masses with the time-of-swing method*, Ph.D. Dissertation (Wuhan: Huazhong University of Science & Technology) (in Chinese)